

SCIENTIFIC REPORTS

OPEN

Involucratusins A–H: Unusual Cadinane Dimers from *Stahlianthus involucratus* with Multidrug Resistance Reversal Activity

Received: 03 March 2016

Accepted: 22 June 2016

Published: 13 July 2016

Qiang-Ming Li*, Jian-Guang Luo*, Rui-Zhi Wang, Xiao-Bing Wang, Ming-Hua Yang, Jun Luo & Ling-Yi Kong

Three novel cadinane dimers, involucratusins A–C (1–3), five unique nor-cadinane-dimers, involucratusins D–H (4–8), together with a known compound (9) were isolated from the rhizomes of *Stahlianthus involucratus*. Their challenging structures and absolute configurations were determined by spectroscopic data, CD experimentation, chemical conversions and single-crystal X-ray diffraction. Compounds 1–3 are unusual cadinane dimers with new connection and novel cores. Compound 4 is a unique nor-cadinane-dimer, and 5 and 6 are two pairs of hemiketal racemates with novel dinor-cadinane-dimer backbone. Compounds 7 and 8 represent unusual dodecanor-cadinane-dimer and tetradecanor-cadinane-dimer carbon skeletons, respectively. The possible biogenetic pathways of 1–8 were proposed, involving nucleophilic addition, S_N2 nucleophilic displacement, [3 + 3] benzannulation, oxidative cleavage, decarboxylation, and oxidative phenol coupling reactions. Multidrug resistance (MDR) reversal activity assay of the isolates were evaluated in doxorubicin-resistant human breast cancer cells (MCF-7/DOX). The combined use of these novel cadinane dimers at a concentration of 10 μM increased the cytotoxicity of doxorubicin by 2.2–5.8-fold. It is the first report about the MDR reversal activity of cadinane dimers.

Sesquiterpenoid dimers are some naturally occurring metabolites that have C_{30} cores, and originate biosynthetically from two sesquiterpenoid molecules¹. Cadinane dimers, as one class of sesquiterpenoid dimers, are of considerable interest due to their ability to induce diverse biological activity (e.g. male antifertility, anticancer, antiviral, and anti-inflammatory)¹. Of these naturally occurring cadinane dimers, most are derived from two units of the corresponding monomers by the free-radical coupling reaction¹, however, rare example that formed by nucleophilic addition reaction have been reported. The occurrence of nor-cadinane-dimer is also surprisingly low, with the only two, aquatidial² and parviflorene³. Recently, we have reported three unprecedented cadinane dimers, involucratusins A–C⁴, from *Stahlianthus involucratus*, a folklore medicine to treat inflammation, pain, and fever⁵, as part of a continued program searching for novel terpenoids from Zingiberaceae plants^{6–9}. These prompt us to perform a further phytochemical investigation on *S. involucratus*. As a result, three unusual cadinane dimers, involucratusins A–C (1–3) (Fig. 1), five novel nor-cadinane-dimers, involucratusins D–H (4–8), and a biosynthetically related known compound parviflorene D (9)^{3,10} were isolated and elucidated. Structurally, the architectures of 1–8 are different from the previously isolated cadinane dimers and nor-cadinane-dimers and represent five new carbon skeletons. Moreover, from the viewpoint of biosynthesis, the key biosynthesis reactions of cadinane dimers 1–3, nucleophilic addition, and nor-cadinane-dimers 5–8, oxidative cleavage, are extremely rare in the biosynthesis of cadinane dimers and norcadinane-dimers, respectively. Herein are described the isolation, structure elucidation and possible biosynthesis of new metabolites 1–8, as well as MDR reversal activities of the compounds obtained.

State Key Laboratory of Natural Medicines, Department of Natural Medicinal Chemistry, China Pharmaceutical University, 24 Tong Jia Xiang, Nanjing 210009, People's Republic of China. *These authors contributed equally to this work. Correspondence and requests for materials should be addressed to L.-Y.K. (email: cpu_lykong@126.com)

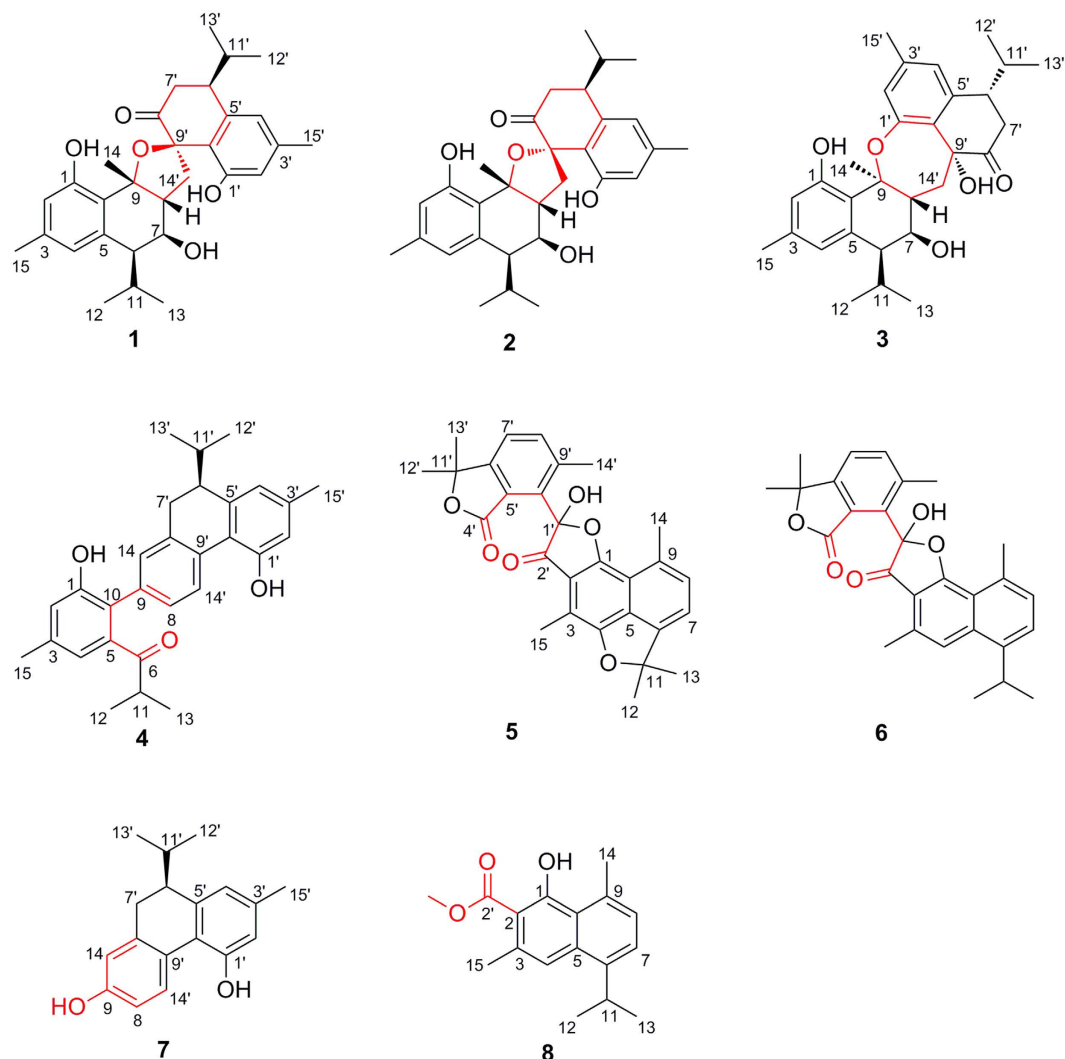


Figure 1. Structures of compounds 1–8.

Results and Discussion

Structure elucidation.

Involucratusin A (**1**) was isolated as white columnar crystals (MeOH:H₂O = 10:1). Its molecular formula C₃₀H₃₈O₅, corresponding to 12 degrees of unsaturation, was established by HRESIMS data (m/z 501.2613 [M+Na]⁺, calcd for C₃₀H₃₈O₅Na, 501.2611). The ¹H NMR spectrum of **1** showed the presence of two 1,2,3,5-tetrasubstituted benzene rings [δ_{H} 6.40 (1H, br s), 6.55 (1H, br s), 6.66 (1H, br s), 6.69 (1H, br s)], two isopropyl groups [δ_{H} 1.95 (1H, m), 1.22 (1H, d, 6.5 Hz), 0.79 (1H, d, 6.5 Hz), 1.84 (1H, m), 0.87 (1H, d, 6.5 Hz), 0.77 (1H, d, 6.5 Hz)] and three tertiary methyls [δ_{H} 2.29 (3H, s), 2.27 (3H, s), 1.92 (3H, s)]. Its ¹³C NMR spectrum displayed a total of thirty carbons that, with the aid of HSQC spectrum, were deduced to contain a ketonic (δ_{C} 207.3), twelve aromatic (δ_{C} 117.1, 117.2, 119.9, 121.6, 123.2, 123.4, 136.4, 137.7, 139.8, 140.4, 155.3, 155.8), and seven methylic carbons (Supplementary Table S1). According to the data above, compound **1** should contain two aromatic cadinane sesquiterpenoid moieties, which was further confirmed by 2D NMR spectra analysis (¹H-¹H COSY correlations: H-2/H-4/H₃-15, H-8/H₂-7/H-6/H-11/H₃-12/H₃-13, H-2'/H-4'/H₃-15', H₂-7'/H-6'/H-11'/H₃-12'/H₃-13'; and HMBC correlations: H-2 with C-4/C-10, H-4 with C-6/C-10, H₃-14 with C-8/C-9/C-10, H₃-15 with C-2/C-3/C-4, H-2' with C-4'/C-10', H-4' with C-6'/C-10', H₂-14' with C-8'/C-9'/C-10', H₃-15' with C-2'/C-3'/C-4') (Fig. 2A).

Further analysis, the carbon-carbon connectivity of two determined cadinane sesquiterpenoid moieties was established by the HMBC correlations from H-8 to C-9' and C-14'; and from H₂-14' to C-7, C-8 and C-9, which was further confirmed by the ¹H-¹H COSY correlations of H-8 with H₂-14'. The remaining four oxygen and three hydrogen atoms in molecular formula were incorporated with the five oxygenated carbons C-1 (δ_{C} 155.3), C-7 (δ_{C} 73.4), C-9 (δ_{C} 90.4), C-1' (δ_{C} 155.8) and C-9' (δ_{C} 91.4) to deduce the presence of three hydroxyl groups and one ether bond. However, due to the absence of the key HMBC correlations, the locations of the hydroxyl groups and ether bond could not be determined to completely establish the planar structure of **1**. After numerous attempts, a single crystal was obtained from MeOH/H₂O (10:1) and subjected to an X-ray diffraction experiment using a mirror Cu K α radiation. Thus, as shown in Fig. 2B, compound **1** was established as a novel cadinane dimer with

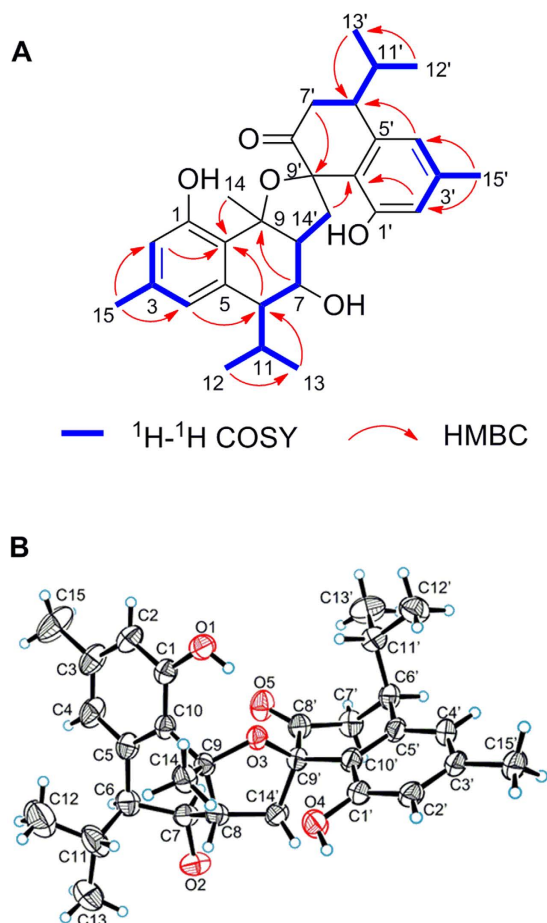


Figure 2. Key HMBC, ^1H - ^1H COSY correlations (A) and X-ray structure (B) of compound **1**.

an unusual 1-oxaspiro[4.5]decane ring and a new manner of bond connection (C-8 and C-14', C-9 and oxygen on C-9') (Fig. 1).

In the ROESY spectrum of **1** (Supplementary Fig. S2), the ROE correlations of H-8 (δ_{H} 2.81) with H-11/H₃-13/H₃-14; H₃-14 (δ_{H} 1.92) with H-11/H₃-13; and H-7 with H-6/H-14'b indicated the relative configurations of C-6, C-7, C-8 and C-9 were *R*^{*}, *R*^{*}, *R*^{*} and *R*^{*}, respectively. However, the relative configurations of C-6' and spiro C-9' were still unable to be established by ROESY spectrum due that both C-8' and C-10' are quaternary carbons and the absence of key correlation of H₂-14' with H-6' or H-11'. The completely relative configuration of **1** was finally established by the successful X-ray diffraction experiment (Fig. 2B). Moreover, the absolute configuration of **1** was also assigned as 6*R*, 7*R*, 8*R*, 9*R*, 6'*S*, 9'*R* by Flack absolute structure parameter $-0.03(9)$.

On the basis of analysis of the MS, 1D, and 2D NMR data (Supplementary Table S1, Fig. S1), involucratustin B (**2**) was shown to possess the same planar structure as **1**. The slight differences in the ^{13}C NMR chemical shifts of C-8', C-9' and C-10' suggested that **2** might be a stereoisomer of **1** at C-9¹¹⁻¹³. In the ROESY spectrum of **2** (Supplementary Fig. S2), the cross-peaks of H-11 with H-8/H₃-14; H-7 with H-6/H-14'b suggested the relative configurations of C-6, C-7, C-8 and C-9 were *R*^{*}, *R*^{*}, *R*^{*} and *R*^{*}, respectively. Although the ROE correlations of H-14'a with H-11'/H₃-12'/H₃-13' deduced the isopropyl at C-6' and CH₂-14' hold same orientation, the relative configurations of the C-6' and spiro C-9' could not be established due to the C-8' and C-10' were quaternary carbons.

To completely determine the relative and absolute configurations of **2**, the ketone at C-8' was reduced to the secondary alcohol to afford the major products **2a** (Fig. 3A and Supplementary Fig. S1, NMR data in Supplementary Table S1). Firstly, the relative configuration of **2a** was established as 6*R*^{*}, 7*R*^{*}, 8*R*^{*}, 9*R*^{*}, 6'*S*^{*}, 8'*S*^{*}, 9'*R*^{*} by the ROE correlations of H-11 with H-8/H₃-14; H-7 with H-6/H-14'b; H-14'a with H-11'/H₃-13'; and H-8' with H-8/H₃-14/H-6' (Supplementary Fig. S2). Subsequently, using the modified Mosher's method^{14,15}, the absolute configurations of C-7 and C-8' of **2a** were determined as *R* and *S*, respectively, on the basis of the analysis of the diagnostic proton chemical shift values (positive $\Delta\delta_{\text{S,R}}$ values for H-8 and H-14'a, and negative $\Delta\delta_{\text{S,R}}$ values for H-6, H-7, H-11, H₃-12, H₃-13, H-6', H-7'b, H-8', H-11', H₃-12' and H₃-13') between protons of the C-7 and C-8' bis-(*S*)- and bis-(*R*)- MTPA esters of **2a** (**2ab** and **2aa**) (Fig. 3B). Thus, the absolute configurations of the chiral centers in **2a** were assigned as 6*R*, 7*R*, 8*R*, 9*R*, 6'*S*, 8'*S*, 9'*R*, respectively. Finally, according to the absolute configuration of **2a** determined above, the absolute configuration of **2** was undoubtedly established as 6*R*, 7*R*, 8*R*, 9*R*, 6'*S*, 9'*S*, which unambiguously confirmed **2** was a stereoisomer of **1** at C-9'.

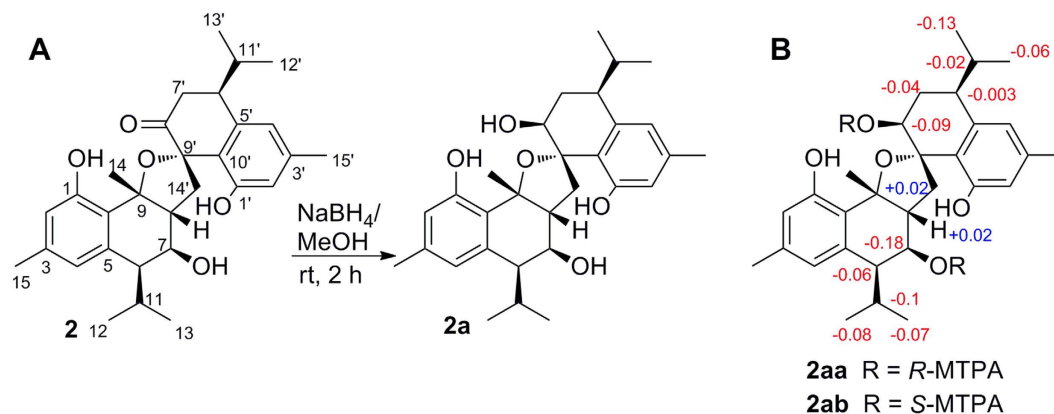


Figure 3. (A) Preparation of compound **2a** from compound **2**; (B) ^1H NMR chemical shift differences of the MTPA ester derivatives of compound **2a**.

Involucratusin C (**3**) was assigned to share the same molecular formula $\text{C}_{30}\text{H}_{38}\text{O}_5$ as **1** and **2** by its HRESIMS data (m/z 501.2610 $[\text{M}+\text{Na}]^+$, calcd for $\text{C}_{30}\text{H}_{38}\text{O}_5\text{Na}$, 501.2611), which deduced **3** might also be a cadinane dimer. The 1D NMR (Supplementary Table S1) of **3** was incorporated with the HMBC spectrum (Supplementary Fig. S1) to show the presence of two cadinane sesquiterpenoid units, which further confirmed that **3** was a cadinane dimer. Further analysis, the HMBC correlations of $\text{H}_2\text{-14}'$ with C-7/C-8/C-9, and H-8 with C-9'/C-14' established the carbon-carbon connectivity of two cadinane sesquiterpenoid moieties of **3**. According to the molecular formula $\text{C}_{30}\text{H}_{38}\text{O}_5$ and the five oxygenated carbons (C-1: δ_{C} 155.8; C-7: δ_{C} 70.7; C-9: δ_{C} 87.4; C-1': δ_{C} 152.2; C-9': δ_{C} 76.1), the remaining four oxygen atoms and three hydrogen atoms indicated the presence of three hydroxyl groups and an ether bond. To determine the position of the hydroxyl groups and ether bond, 1D and 2D NMR spectra of **2** were recorded in DMSO- d_6 . The HMBC correlations of the hydroxyl proton at δ_{H} 8.90 with C-1/C-2/C-10; the hydroxyl proton at δ_{H} 4.95 with C-6/C-7/C-8; and the hydroxyl proton at δ_{H} 5.26 with C-8'/C-9'/C-10'/C-14' suggested the hydroxyl groups located at C-1, C-7 and C-9', respectively, and the ether bond linked with C-9 and C-1' to form a novel seven-membered cyclic ether. Thus, the planar structure of compound **3** was deduced as a novel seven-membered cyclic ether cadinane dimer with new manner of bond connection (C-8 and C-14', C-9 and oxygen on C-1') (Fig. 1).

In the ROESY spectrum (Supplementary Fig. S2), the cross-peaks of H-8 with OH-7/H-11/H₃-12/H₃-13; OH-7 with H-11; and H-7 with H-6/H₃-14/H-14'b indicated the relative configurations of the chiral centers C-6, C-7, C-8 and C-9 were R^* , R^* , R^* and S^* , respectively. The relative configurations of C-6' and C-9' were deduced as S^* and R^* by the ROE correlations of OH-9' with H₃-14/H-11'/H₃-13'/H-14'b; H-7'b with H-11'/H₃-13', and H-7' a with H-14'a. Having assigned the relative configuration of **3**, we next attempted to determine the absolute configuration via a modified Mosher's method^{14,15}. The absolute configuration of C-7 was established to be R by the analysis of the diagnostic proton chemical shift values (positive $\Delta\delta_{S-R}$ values for H-8, H-6', H₂-7', H₃-12', H₃-13' and H-14'a, and negative $\Delta\delta_{S-R}$ values for H-7, H-11 and H₃-12) between protons of the C-7 (S)- and (R)-MTPA esters of **3** (**3b** and **3a**) (Fig. 4), although an anomalous positive $\Delta\delta_{S-R}$ value for H-6 appeared. The reason of the irregularity of H-6 would be the conformation of the MTPA moieties slightly different from the ideal one, which might be owing to the compression of other groups in **3a** and **3b**^{16–18}. Combining with the relative configuration established above, the absolute stereochemistry of **3** was determined as $6R, 7R, 8R, 9S, 6'S, 9'R$.

Involucratusin D (**4**) was obtained as a yellowish oil, and was deduced to hold the molecular formula $\text{C}_{29}\text{H}_{32}\text{O}_3$ by its HRESIMS data (m/z 451.2245 $[\text{M}+\text{Na}]^+$, calcd for $\text{C}_{29}\text{H}_{32}\text{O}_3\text{Na}$, 451.2244), revealing **4** might be a nor-cadinane-dimer. From the 1D NMR data (Supplementary Table S2), the presence of two 1,2,3,5-tetrasubstituted and one 1,2,4-trisubstituted benzene rings were deduced by three groups of signals at δ_{H} 6.91 (br s) and 6.81 (br s), and at 6.59 (br s) and 6.62 (br s), and at 7.20 (br d, 8.0), 8.28 (br d, 8.0) and 7.15 (br s) in the ^1H NMR incorporating with the eighteen aromatic carbons in the ^{13}C NMR. Interpretation of the ^1H - ^1H COSY and HSQC spectra led to the assignment of an isopropyl group (H-11/H₃-12/H₃-13) and an isopentane group (H₂-7'/H-6'/H-11'/H₃-12'/H₃-13') (Supplementary Fig. S1). These five substructures combining with the remaining two methyl groups [δ_{H} 2.31 (s), δ_{C} 21.3; δ_{H} 2.37 (s), δ_{C} 21.4] and one carbonyl group (δ_{C} 211.7) were connected by the key HMBC correlations of H-4 with C-6; H-11 with C-5/C-6; H₃-15 with C-2/C-3/C-4; H-8 with C-10; H-14 with C-10/C-7'; H-6' with C-4'/C-5'/C-8'/C-10'; H₂-7' with C-14/C-5'/C-8'/C-9'; H-14' with C-10'; H₃-15' with C-2'/C-3'/C-4' to establish the novel aromatic 6,7-seco-7-nor-cadinane-dimer carbon skeleton. The oxygenated aromatic carbons C-1 (δ_{C} 152.8) and C-1' (δ_{C} 153.2) were incorporated with the remaining two oxygen and two hydrogen atoms in molecular formula to indicate the presence of OH-1 and OH-1'. Thus, the unusual planar structure of **4** was established as shown in Fig. 1.

The absolute configuration at C-6' of **4** was determined by application of the exciton chirality method^{19–21}. The positive split [$\Delta\epsilon$ +35.1 (237 nm), -18.5 (210 nm)] in CD spectrum of **4** (Fig. 5) indicated the clockwise screw sense between the two long axes of the phenyl chromophores, leading to the establishment of the $6'S$ configuration in **4**.

Involucratusin E (**5**) was obtained as lamellar crystals (MeOH:H₂O = 10:1). The pseudomolecular ion at m/z 459.1804 $[\text{M}+\text{H}]^+$ (calcd for $\text{C}_{28}\text{H}_{27}\text{O}_6$, 459.1802) in the HRESIMS of compound **5** determined that it possessed

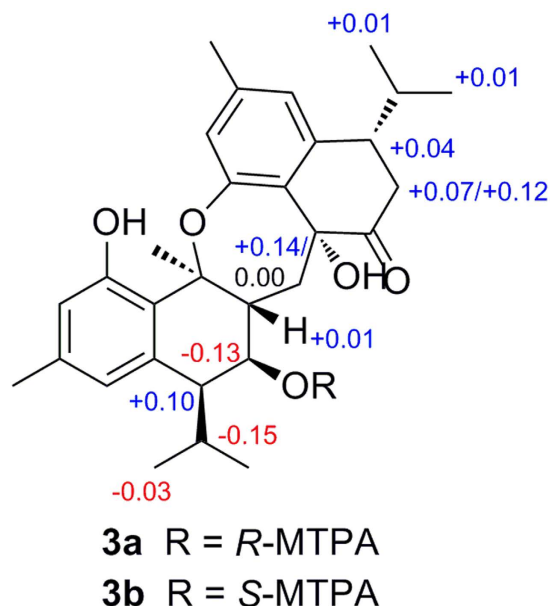


Figure 4. ^1H NMR chemical shift differences of the MTPA ester derivatives of compound 3.

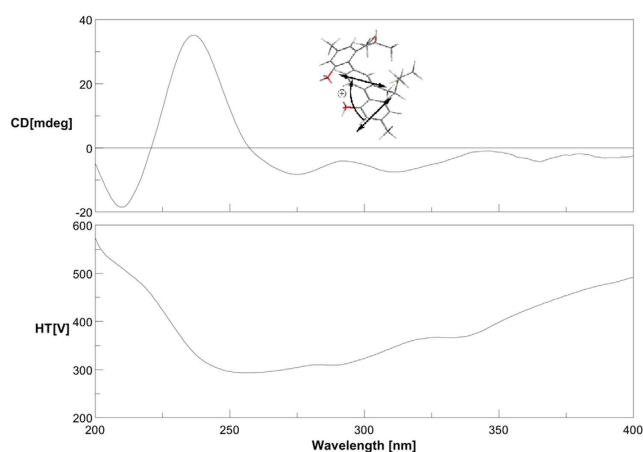


Figure 5. CD and exciton chirality sign of compound 4.

a molecular formula of $\text{C}_{28}\text{H}_{26}\text{O}_6$, which indicated **5** might be a dinor-cadinane-dimer. The ^1H NMR spectrum of **5** showed seven singlet methyls, and two pairs of *ortho*-coupled aromatic doublets [$\delta_{\text{H}} = 7.23, 7.15$ (each 1H, d, $J = 7.0$ Hz)] and [$\delta_{\text{H}} = 7.48, 7.31$ (each 1H, d, $J = 8.0$ Hz)] (Supplementary Table S2). On the basis of ^{13}C NMR and HSQC spectra, compound **5** showed 28 carbons, including two carbonyl carbons ($\delta_{\text{C}} 173.2, 198.7$) and sixteen aromatic carbons. From the 1D NMR data above, the presence of 1,2,3,4,5,8-hexasubstituted naphthalene and 1,2,3,4-tetrasubstituted benzene moieties were established. Further analysis, the HMBC correlations of $\text{H}_3\text{-}12/\text{H}_3\text{-}13$ with C-6/C-11; $\text{H}_3\text{-}14$ with C-8/C-9/C-10; $\text{H}_3\text{-}15$ with C-2/C-3/C-4, $\text{H}_3\text{-}12'/\text{H}_3\text{-}13'$ with C-6'/C-11'; $\text{H}_3\text{-}14'$ with C-8'/C-9'/C-10'; and OH-1' with C-1'/C-2'/C-10' (Fig. 6A) indicated the presence of an aromatic cadinane and a dinorcadinane sesquiterpenoid unit, which further confirmed **5** was an aromatic dinor-cadinane-dimer. However, due to the crowded quaternary carbons, the connection of the aromatic cadinane and dinorcadinane sesquiterpenoid units could not be determined by NMR spectra to establish the complete structure of **5**. Finally, a single crystal suitable for X-ray analysis was obtained after careful recrystallization and subjected to an X-ray diffraction experiment to determine the structure of **5** as an unique 3',4'-*seco*-3',15'-dinor-cadinane-dimer (Fig. 6B). However, the optical rotation value of **5** was found to be zero indicating **5** was a racemic mixture, which was further confirmed by crystallographic data analysis^{22,23}. Subsequent separation on a chiral preparative HPLC for two enantiomers was not successful, due to the reversible nature of hemiketal at the only chiral center C-1'^{24,25}.

Involucratusin F (**6**) was isolated as yellowish amorphous powder. HRESIMS data (m/z 445.2011 [$\text{M}+\text{H}$] $^+$, calcd for $\text{C}_{28}\text{H}_{29}\text{O}_5$, 445.2010) gave the molecular formula $\text{C}_{28}\text{H}_{28}\text{O}_5$ deducing **6** has a similar dinor-cadinane-dimer structure. This deduction was corroborated by the semblable NMR data of **5** and **6** (Supplementary Table S2). However, the C-4 [$\delta_{\text{H}} 7.50$ (1H, s), $\delta_{\text{C}} 118.9$] and C-11 [$\delta_{\text{H}} 3.64$ (1H, m), $\delta_{\text{C}} 29.1$] of **6**

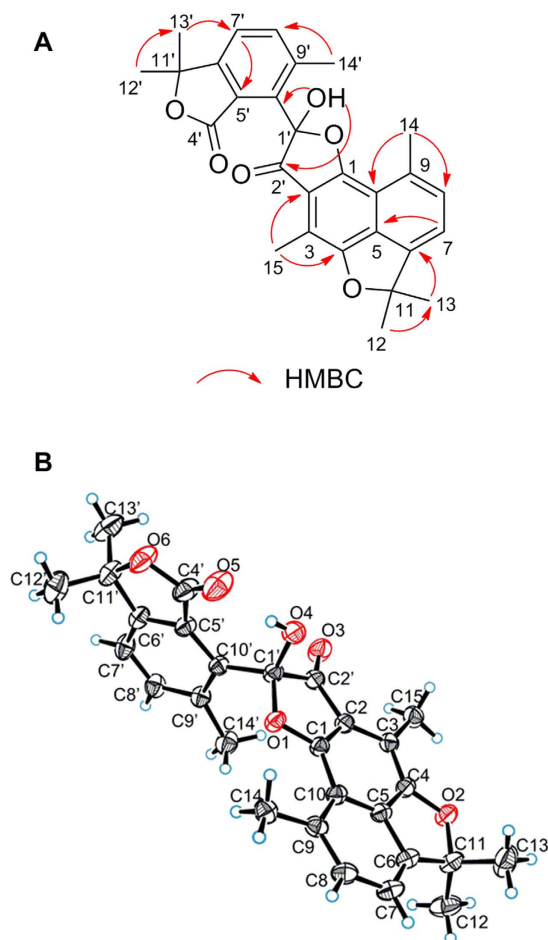


Figure 6. Key HMBC correlations (A) and X-ray structure (B) of compound 5.

were different from the oxygenated quaternary carbons C-4 (δ_C 152.2) and C-11 (δ_C 92.5) of 5 indicating the ether bond between C-4 and C-11 of 5 have disappeared in 6, which was supported by the HMBC correlations: H-4 with C-2/C-6/C-10/C-15; and H-11 with C-5/C-6/C-7/C-12/C-13 (Supplementary Fig. S1). Thus, the structure of 6 was also determined to be a novel 3',4'-seco-3',15'-dinor-cadinane-dimer (Fig. 1). The zero optical rotation value revealed 6 also was a racemic mixture.

Involucratusin G (7), with a molecular formula $C_{18}H_{20}O_2$ deduced by its HRESIMS data (m/z 267.1390 $[M-H]^-$, calcd for $C_{18}H_{19}O_2$, 267.1391), was obtained as a yellowish oil. The 1D NMR spectra (Supplementary Table S3), with the help of HSQC spectrum, revealed 7 contained a 1,2,3,5-tetrasubstituted benzene ring [δ_H 6.57 (br s), 6.59 (br s); δ_C 115.9, 118.3, 123.2, 136.8, 143.0, 152.4] and a 1,2,4-trisubstituted benzene ring [δ_H 6.73 (br d, 9.0), 6.74 (br s), 7.97 (d, 9.0); δ_C 113.2, 116.0, 125.8, 127.9, 139.1, 154.4]. The presence of an isopropyl group were deduced by the characteristic 1H NMR signals [δ_H 1.41 (H-11, m); 0.77 (H₃-12, d, 6.5); 0.87 (H₃-13, d, 6.5)]. Further analysis, the three aforementioned substructures were incorporated with one methyl, one methylene and one methine groups to form the unique dodecanor-cadinane-dimer carbon skeleton of 7 according to the HMBC correlations of H-4'/H₃-12'/H₃-13' with C-6'; H₂-7' with C-14/C-5'/C-8'/C-9'; H-14' with C-10'; and H₃-15' with C-2'/C-3'/C-4' (Supplementary Fig. S1). The oxygenated aromatic carbons C-9 (δ_C 154.4) and C-1' (δ_C 152.4) and the remaining two oxygen and two hydrogen atoms in molecular formula indicated the presence of OH-9 and OH-1'. Thus, the planar structure of 7 was established as a novel dodecanor-cadinane-dimer (Fig. 1).

The absolute configuration of 7 was assigned by a CD exciton chirality method^{19–21}. In the CD spectrum of 7 (Fig. 7), a positive Cotton effect at 235 nm ($\Delta\epsilon$ +46.4) and a negative Cotton effect at 214 nm ($\Delta\epsilon$ -25.2) due to the transition interaction between two identical phenyl chromophores indicated a positive chirality for 7, which suggested the transition dipole moments of the two chromophores were oriented in a clockwise manner. Thus, the absolute configuration of 7 was established as 6'S.

Involucratusin H (8), which of molecular formula $C_{17}H_{20}O_3$ was deduced by its HRESIMS data (m/z 273.1486 $[M+H]^+$, calcd for $C_{17}H_{21}O_3$, 273.1485), was obtained as yellowish needle crystals (MeOH:H₂O = 10:1). The 1H NMR spectrum of 8 (Supplementary Table S3) gave altogether four methyls, one methoxyl, one phenolic hydroxyl, one aliphatic methine, and three aromatic methines [δ_H 7.14 (d, 7.5), 7.32 (s), 7.34 (d, 7.5)]. Its ^{13}C NMR spectrum revealed a total of seventeen carbons including one ester carbonyl (δ_C 173.9) and ten aromatic carbons. In this molecule, the presence of 1,2,3,5,8-pentasubstituted naphthalene moiety was deduced based on the aforementioned three aromatic protons and ten aromatic carbons. From the HMBC spectrum (Supplementary Fig. S1),

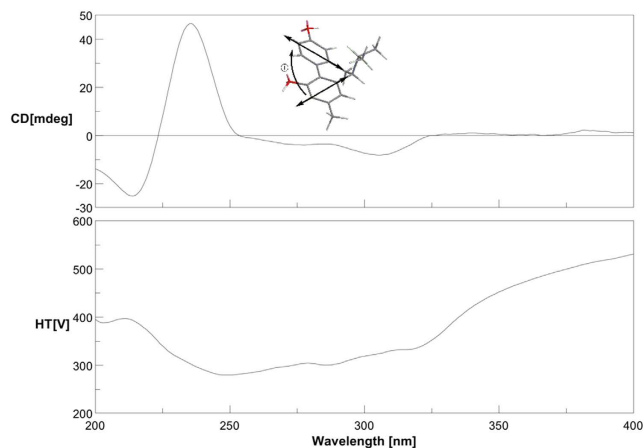


Figure 7. CD and exciton chirality sign of compound 7.

the correlations of H₃-12/H₃-13 with C-6/C-11; H₃-14 with C-8/C-9/C-10; and H₃-15 with C-2/C-3/C-4 were incorporated the naphthalene moiety deduced above to established the aromatic cadinane sesquiterpenoid unit. Furthermore, the HMBC correlations from the phenolic hydroxyl (δ_{H} 13.11) to C-2, C-10 and C-2' (δ_{C} 173.9); and from the methoxyl (δ_{H} 3.99) to C-2' deduced the phenolic hydroxyl linking at C-1 and the methyl ester group linking at C-2. To further confirm the deduced above, as showed in Supplementary Fig. S3, the single crystals of **8** were obtained and subjected to an X-ray diffraction experiment. Thus, the structure of **8** was doubtless determined as a novel tetradecanor-cadinane-dimer (Fig. 1).

Biosynthetic pathway. Comparing with the reported cadinane dimers^{1,4}, involucratustones A–H (**1–8**) represent five new carbon skeletons. The skeleton of **1–3** is corresponded to novel cadinane sesquiterpenoid dimer with unusual 1-oxaspiro[4.5]decane ring (**1** and **2**) or seven-membered cyclic ether ring (**3**), and new manners of bond connection (**1** and **2**: C-8 and C-14', C-9 and oxygen on C-9'; **3**: C-8 and C-14', C-9 and oxygen on C-1'). Although a series of cadinane dimers have been reported from natural sources, hitherto, only two nor-cadinane-dimers have been isolated^{1–3}. Nor-cadinane-dimer (**4**), dinor-cadinane-dimer (**5** and **6**), dodecanor-cadinane-dimer (**7**), and tetradecanor-cadinane-dimer (**8**) represent four novel nor-cadinane-dimer carbon skeletons, which greatly enrich the structure of nor-cadinane-dimer. The novel and various backbones of **1–8** prompted us to speculate their biosynthetic pathways. As shown in Fig. 8, the pathways of **1–8** originating from cadalenequinone, which was considered as the biosynthetic monomeric precursor of involucratustones A–C⁴, were presumed, in which nucleophilic addition^{9,26}, S_N2 nucleophilic displacement²⁷, [3 + 3] benzannulation²⁸, oxidative cleavage²⁹, decarboxylation^{30,31}, oxidative phenol coupling³² were included.

From the viewpoint of biosynthesis, the most reported cadinane dimers are formed by the free-radical coupling reaction of two units of the corresponding monomers¹. However, the backbone of involucratustones A–C (**1–3**) was proposed to be generated by the key nucleophilic addition reaction, which indicated **1–3** would provide new insight into the mechanisms of cadinane dimer biosynthesis. In the Fig. 8, it is revealed that the formation of nor-cadinane-dimer **4** is attributed to the decarboxylation reaction, which is the most common biogenetic pathway to form norterpenoids^{2,9,33–35}. However, interesting, different from the most norterpenoids, the carbon skeletons of dinor-cadinane-dimers **5** and **6**, dodecanor-cadinane-dimer **7**, and tetradecanor-cadinane-dimer **8** were speculated to be produced by the key oxidative cleavage reaction. This indicated the elucidation of **5–8** would be a useful inspiration for the biosynthesis and total synthesis investigation of norterpenoids.

MDR reversal activity screening. To search for effective MDR reversal agents, the MDR reversal activities of compound **1**, **2**, **4**, **5**, **7–9** were evaluated in MCF-7/DOX cells using the MTT method. The cytotoxicity assay exhibited that they were noncytotoxic to MCF-7/DOX cells, while they enhanced the cytotoxicity of DOX by 2.2–5.8-fold when incorporated at 10 μM (Supplementary Table S4). Among them, compound **1** and **2** exhibited higher reversal fold (5.8 and 4.1, respectively), and **1** slightly higher than **2**. These results indicated that the characteristic 1-oxaspiro[4.5]decane ring of **1** and **2** might be a beneficial group for their MDR reversal activities, and the different configuration at spiro C-9' of 1-oxaspiro[4.5]decane ring in **1** and **2** should slightly affect their activities. Cadinane dimers were reported to have a broad spectrum of biological activities such as male antifertility, anticancer, antiviral, and anti-inflammatory¹. However, it is the first time that the MDR reversal activities of cadinane dimers have been reported. Therefore, the MDR reversal activities of the isolates would exploit new dimension for the bioactivity research of cadinane dimer.

In conclusion, the challenging structures of eight novel cadinane dimers and nor-cadinane-dimers, involucratustones A–H (**1–8**), from the rhizomes of *S. involucratu* were established by a combination of spectroscopic data, CD experimentation, chemical reactions and single-crystal X-ray diffraction. Compounds **1–3** represent novel cadinane dimer backbone with new connection and unusual cores. Compounds **4–8** are a series of novel nor-cadinane-dimers representing four new carbon skeletons. Moreover, the key biogenetic reactions of cadinane dimers **1–3**, nucleophilic addition, and nor-cadinane-dimers **5–8**, oxidative cleavage, are very rare during the naturally formative process of cadinane dimers and norterpenoids, respectively. Therefore, the isolation of

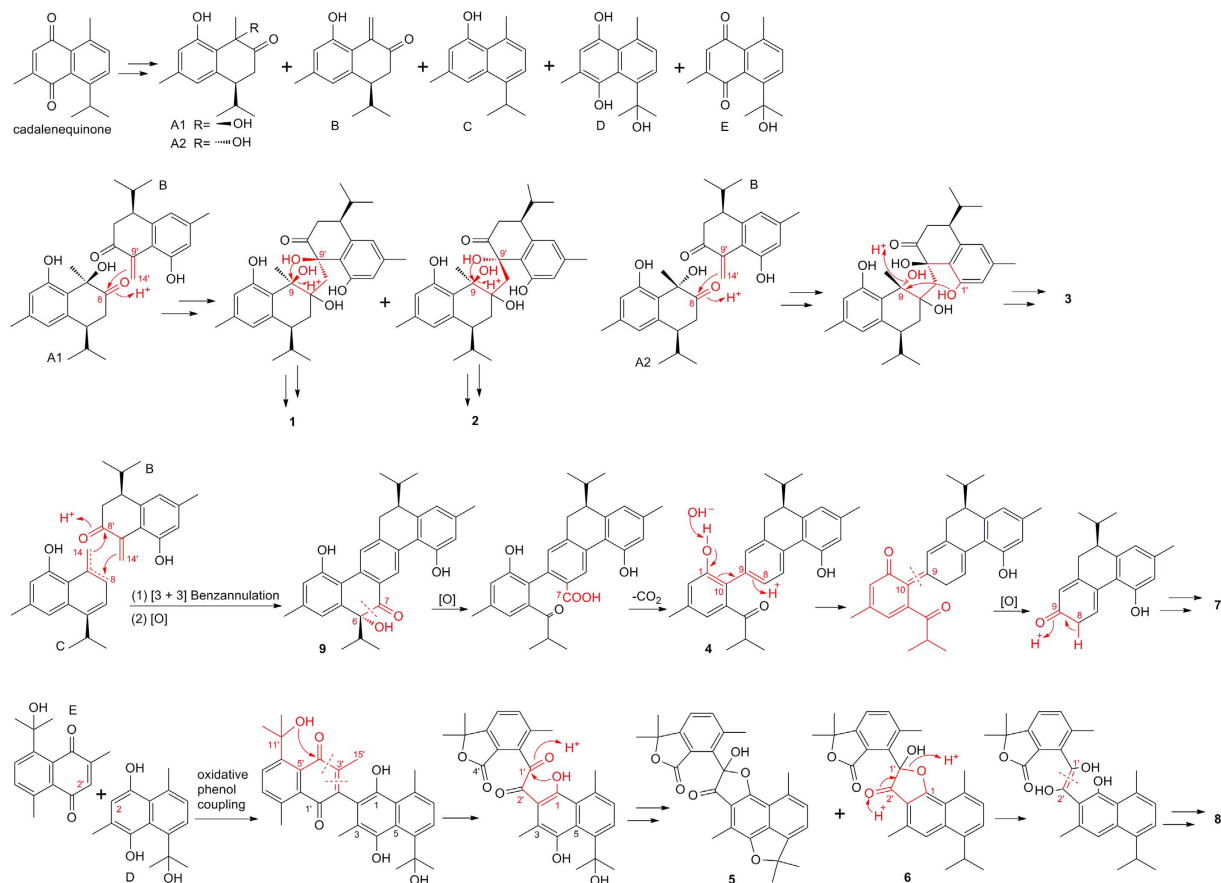


Figure 8. Plausible Biosynthetic Pathways for compounds 1–8.

1–8 has yielded advantageous illuminations for the research of cadinane dimer and norterpeneoid biosynthesis. Biologically, the MDR reversal activities of 1, 2, 4, 5, 7–9 were evaluated in MCF-7/DOX cells. The results indicated that they enhanced the cytotoxicity of DOX by 2.2–5.8-fold when incorporated at 10 μ M. It is the first report about the MDR reversal activity of cadinane dimers. Thus, the MDR reversal activities of the isolates would expand new dimension for the bioactivity research of cadinane dimer, and provide valuable inspiration for the MDR reversal drug discovery.

Methods

General experimental procedures. Melting point was measured on an X-4 digital display micro-melting apparatus, uncorrected. Optical rotations were determined with a JASCO P-1020 polarimeter. UV spectra were performed on a Shimadzu UV-2450 spectrophotometer. CD spectrum was measured on a JASCO 810 spectropolarimeter. 1D and 2D NMR spectra were acquired on a Bruker AV-500 NMR instrument at 500 MHz (1 H) and 125 MHz (13 C) in CDCl_3 and $\text{DMSO}-d_6$. ESI and HRESI mass spectra were recorded on an Agilent 1100 series LC-MSD-Trap-SL mass analyzer and an Agilent 6520B Q-TOF mass instrument, respectively. Column chromatography (CC) was done with Silica gel (Qingdao Haiyang Chemical Co., Ltd., Qingdao, China), ODS (40–63 μ m, Fuji, Japan), Sephadex LH-20 (Pharmacia, Sweden). Preparative HPLC was carried out using an SHMADZU LC-6AD series instrument with a Shim-park RP-C18 column (20 \times 200 mm) and a SHMADZU SPD-20A detector.

Plant material. The rhizomes of *S. involucratus* were collected from Guangxi province of China in November 2012, and were authenticated by Professor Min-Jian Qin, Department of Medicinal Plants, China Pharmaceutical University. A voucher specimen (No. 201211-SI) is deposited in the Department of Natural Medicinal Chemistry, China Pharmaceutical University.

Extraction and isolation. The air-dried rhizomes of *S. involucratus* (5 kg) were exhaustively extracted with 95% EtOH at room temperature (5 \times 1 d). The residue (200 g) obtained by concentrating the EtOH extract under reduced pressure was suspended in H_2O (1.5 L), then partitioned successively with petroleum ether (PE) (4 \times 2 L), dichloromethane (CH_2Cl_2) (4 \times 2 L) and ethyl acetate (EtOAc) (4 \times 2 L). The PE, CH_2Cl_2 and EtOAc extracts yielded 120 g, 30 g and 4 g after removal of the solvent, respectively. The CH_2Cl_2 extract was chromatographed on a silica gel column using a gradient of PE-acetone (10:1, 5:1, 2:1, 1:1) to afford four fractions (Fr. 1–4) collected and pooled on the basis of TLC analysis. Fr. 1 (4.7 g) was run on ODS column chromatography with $\text{MeOH}-\text{H}_2\text{O}$

(50–100%), to obtain eight fractions (Fr. 1.1–Fr. 1.8). Fr. 1.3 was then chromatographed on an ODS column using a step gradient of MeOH–H₂O (60–100%), to give sixteen fractions (Fr. 1.3.1–1.3.16). Fr. 1.3.8 was further purified on preparative HPLC using MeOH–H₂O (80:20, 10 mL/min) to obtain **2** (31 mg) and **6** (2 mg). Fr. 1.3.13 was recrystallized with MeOH/H₂O (10:1), yielding **8** (2 mg). Fr. 2 (9.3 g) was run on ODS column chromatography with MeOH–H₂O (30–100%), to obtain five fractions (Fr. 2.1–Fr. 2.5). Fr. 2.2 was performed on a silica gel column chromatography using a gradient of PE–acetone (10:1, 5:1, 2:1) to afford seven fractions (Fr. 2.2.1–2.2.7). Fr. 2.2.2 was then chromatographed on an ODS column using a step gradient of MeOH–H₂O (50–100%), to give twelve fractions (Fr. 2.2.2.1–2.2.2.12). Fr. 2.2.2.5 was run on Sephadex LH-20 with MeOH, to obtain eight subfractions (Fr. 2.2.2.5.1–2.2.2.5.8). Fr. 2.2.2.5.1 was finally purified on preparative HPLC using MeOH–H₂O (85:15, 10 mL/min) to obtain **3** (4 mg). Fr. 2.2.2.5.2 was recrystallized with MeOH/H₂O (10:1) to yield **1** (50 mg). Fr. 2.2.2.6 was purified by Sephadex LH-20 column chromatography and recrystallized with MeOH/H₂O (10:1) to obtain **5** (18 mg). After chromatographed on an ODS column using a step gradient of MeOH–H₂O (65–100%), Fr. 2.2.4 was separated to give twelve fractions (Fr. 2.2.4.1–2.2.4.12). Fr. 2.2.4.2 was purified by Sephadex LH-20 column chromatography and preparative HPLC (MeOH/H₂O = 80:20, v/v) to obtain **4** (6 mg), **7** (2 mg) and **9** (100 mg).

Spectroscopic data. Involucratusin A (**1**): colorless needle crystals (MeOH/H₂O, 10:1); mp 187–190 °C; $[\alpha]_D^{25} + 82.0$ (*c* 0.2, MeOH); UV (MeOH) (log ϵ) λ_{\max} : 207 (4.71) nm, 283 (3.64) nm; CD (MeOH): λ (ϵ) = 207 (2.26), 219 (13.88), 277 (−3.48), 301 (−3.40) nm; for ¹H and ¹³C NMR data, see Supplementary Table S1; ESIMS *m/z* 513.2 [M+Cl][−]; HRESIMS *m/z* 501.2613 [M+Na]⁺ (calcd for C₃₀H₃₈O₅Na, 501.2611).

Involucratusin B (**2**): white amorphous powder; $[\alpha]_D^{25} - 5.4$ (*c* 0.1, MeOH); UV (MeOH) (log ϵ) λ_{\max} : 205 (4.49) nm, 281 (3.68) nm; CD (MeOH): λ (ϵ) = 200 (8.38), 218 (−0.01), 257 (0.33), 283 (−1.16) nm; for ¹H and ¹³C NMR data, see Supplementary Table S1; ESIMS *m/z* 477.2 [M−H][−]; HRESIMS *m/z* 501.2609 [M+Na]⁺ (calcd for C₃₀H₃₈O₅Na, 501.2611).

Involucratusin C (**3**): yellowish oil; $[\alpha]_D^{25} + 138.0$ (*c* 0.2, MeOH); UV (MeOH) (log ϵ) λ_{\max} : 205 (4.27) nm, 283 (3.39) nm; CD (MeOH): λ (ϵ) = 209 (29.72), 230 (15.52), 254 (0.33), 282 (3.96) nm; for ¹H and ¹³C NMR data, see Supplementary Table S1; ESIMS *m/z* 513.3 [M+Cl][−]; HRESIMS *m/z* 501.2610 [M+Na]⁺ (calcd for C₃₀H₃₈O₅Na, 501.2611).

Involucratusin D (**4**): yellowish oil; $[\alpha]_D^{25} - 15.3$ (*c* 0.18, MeOH); UV (MeOH) (log ϵ) λ_{\max} : 213 (4.35) nm, 260 (3.84) nm, 282 (3.88) nm, 316 (3.98) nm; CD (MeOH): λ (ϵ) = 210 (−18.57), 237 (35.11), 275 (−8.30), 312 (−7.52) nm; for ¹H and ¹³C NMR data, see Supplementary Table S2; ESIMS *m/z* 427.4 [M−H][−]; HRESIMS *m/z* 451.2245 [M+Na]⁺ (calcd for C₂₉H₃₂O₃Na, 451.2244).

Involucratusin E (**5**): yellowish needle crystals (MeOH/H₂O, 10:1); mp 256–260 °C; $[\alpha]_D^{25} 0$ (*c* 0.2, MeOH); UV (MeOH) (log ϵ) λ_{\max} : 206 (4.59) nm, 222 (4.61) nm, 280 (4.38) nm, 329 (3.51) nm, 434 (3.73) nm; for ¹H and ¹³C NMR data, see Supplementary Table S2; ESIMS *m/z* 457.1 [M−H][−]; HRESIMS *m/z* 459.1804 [M+H]⁺ (calcd for C₂₈H₂₇O₆, 459.1802).

Involucratusin F (**6**): yellowish amorphous powder; $[\alpha]_D^{25} 0$ (*c* 0.1, MeOH); UV (MeOH) (log ϵ) λ_{\max} : 206 (4.48) nm, 266 (4.45) nm, 290 (3.85) nm, 397 (3.52) nm; for ¹H and ¹³C NMR data, see Supplementary Table S2; ESIMS *m/z* 445.2 [M+H]⁺; HRESIMS *m/z* 445.2011 [M+H]⁺ (calcd for C₂₈H₂₉O₅, 445.2010).

Involucratusin G (**7**): yellowish oil; $[\alpha]_D^{25} 37.8$ (*c* 0.1, MeOH); UV (MeOH) (log ϵ) λ_{\max} : 213 (3.97) nm, 278 (3.67) nm, 298 (3.55) nm; CD (MeOH): λ (ϵ) = 214 (−25.28), 235 (46.47), 305 (−8.15) nm; for ¹H and ¹³C NMR data, see Supplementary Table S3; HRESIMS *m/z* 267.1390 [M−H][−] (calcd for C₁₈H₁₉O₂, 267.1391).

Involucratusin H (**8**): yellowish needle crystals (MeOH/H₂O, 10:1); mp 132–134 °C; UV (MeOH) (log ϵ) λ_{\max} : 219 (4.04) nm, 252 (4.22) nm, 285 (3.35) nm, 296 (3.32) nm, 364 (3.37) nm; for ¹H and ¹³C NMR data, see Supplementary Table S3; HRESIMS *m/z* 273.1486 [M+H]⁺ (calcd for C₁₇H₂₁O₃, 273.1485).

X-ray crystallographic analysis. Crystal data were obtained on a Bruker Smart-1000 CCD with a graphite monochromator with Cu K α radiation ($\lambda = 1.54184 \text{ \AA}$) at 291(2) K. The structures were solved by direct methods using the SHELXS-97 and expanded using difference Fourier techniques, refined with the SHELXL-97. Colorless needle crystals of **1** were obtained from MeOH/H₂O (10:1), two molecules of H₂O was resolved together with **1** in the crystal structure. Crystal data of **1**: C₃₀H₄₂O₇ (*M* = 514.63); orthorhombic crystal (0.36 × 0.32 × 0.25 mm); space group C2; unit cell dimensions *a* = 25.8671(4) Å, *b* = 8.8460(2) Å, *c* = 13.4719(2) Å, *V* = 3082.13(10) Å³; *Z* = 4; *D*_{calcd} = 1.109 mg/mm³; $\mu = 0.630 \text{ mm}^{-1}$; 11127 reflections measured (6.836 ≤ 2 θ ≤ 139.05); 4849 unique (*R*_{int} = 0.0226) which were used in all calculations; the final refinement gave *R*₁ = 0.0502 (> 2 σ (*I*)) and *wR*₂ = 0.1435 (all data); Flack parameter = −0.03(9). Crystallographic data for **1** have been deposited in the Cambridge Crystallographic Data Centre (deposition number: CDCC 1455606).

Yellowish needle crystals of **5** were obtained from MeOH/H₂O (10:1). Crystal data of **5**: C₂₈H₂₆O₆ (*M* = 458.49); orthorhombic crystal (0.35 × 0.3 × 0.26 mm); space group Pbca; unit cell dimensions *a* = 11.94950(10) Å, *b* = 13.38660(10) Å, *c* = 30.6047(2) Å, *V* = 4895.62(6) Å³; *Z* = 8; *D*_{calcd} = 1.244 mg/mm³; $\mu = 0.712 \text{ mm}^{-1}$; 37529 reflections measured (10.366 ≤ 2 θ ≤ 139.804); 4609 unique (*R*_{int} = 0.0227) which were used in all calculations; the final refinement gave *R*₁ = 0.0376 (> 2 σ (*I*)) and *wR*₂ = 0.1082 (all data). Crystallographic data for **5** have been deposited in the Cambridge Crystallographic Data Centre (deposition number: CDCC 1455607).

Yellowish needle crystals of **8** were obtained from MeOH/H₂O (10:1). Crystal data of **8**: C₁₇H₂₀O₃ (*M* = 272.33); orthorhombic crystal (0.36 × 0.32 × 0.3 mm); space group Pna2₁; unit cell dimensions *a* = 19.9103(7) Å, *b* = 10.4660(3) Å, *c* = 7.1348(3) Å, *V* = 1486.76(9) Å³; *Z* = 4; *D*_{calcd} = 1.217 mg/mm³; $\mu = 0.660 \text{ mm}^{-1}$; 9807 reflections measured (8.882 ≤ 2 θ ≤ 138.982); 2441 unique (*R*_{int} = 0.0236) which were used in all calculations; the final refinement gave *R*₁ = 0.0547 (> 2 σ (*I*)) and *wR*₂ = 0.1710 (all data); Flack parameter = −0.3(8). Crystallographic data for **8** have been deposited in the Cambridge Crystallographic Data Centre (deposition number: CDCC 1455608).

Reduction of compound 2 to yield 2a. Approximately 10.0 mg **2** and 10.0 mg NaBH₄ were mixed in 4 ml MeOH at room temperature for 1 h. Further 0.5 ml 0.1 mol/L HCl was added to the reaction mixture for 20 min. The reaction mixture was partitioned with EtOAc (3 × 10 mL), and the organic phase was evaporated and purified by Pre-HPLC using ACN-H₂O (75:25, 10 mL/min) to afford **2a** (8 mg).

Bis-MTPA esters of compound 2a. A 6 μL portion of (S)-MTPACl was added to a solution of **2a** (2 mg) in freshly distilled dry pyridine (0.2 mL), and the mixture was kept at room temperature for 2 h. The reaction mixture was diluted with MeOH, and purified by preparative HPLC using MeOH-H₂O (90:10, 10 mL/min) to afford the bis-(R)-MTPA ester **2aa** (1.7 mg). In the same manner, compound **2a** (2 mg) was treated with (R)-MTPACl to give the bis-(S)-MTPA ester **2ab** (1.6 mg).

Bis-MTPA esters of compound 3. Compound **3** (1.5 mg) was dissolved in freshly distilled dry pyridine (0.2 mL), and 6 μL portion of (S)-MTPACl was added. After kept for 2 h at room temperature, the reaction mixture was diluted with MeOH, and purified by preparative HPLC using MeOH-H₂O (90:10, 10 mL/min) to afford the (R)-MTPA ester **3a** (1.2 mg). S-MTPA ester **3b** (1.2 mg) was prepared with (R)-MTPACl in the same manner.

Cytotoxicity assays. MCF-7/DOX cells were cultured in DMEM medium with 10% fetal bovine serum, harvested with trypsin, and resuspended in a final concentration of 4.5 × 10⁴ cells/mL. Aliquots (0.1 mL) of cell suspension were seeded evenly into 96-well culture multiplates and incubated in a 37 °C incubator containing 5% CO₂ for 24 h. A series of concentrations for the isolates in DMSO were added to designated wells. After 48 h, an MTT assay was performed as described previously³⁶.

MDR reversal assays. MCF-7/DOX cells were distributed into 96-well culture plates at 4.5 × 10³ cells per well. A full range of concentrations of DOX with or without 10 μM samples or 10 μM Verapamil (positive control) were added to the cells. After 48 h, the MTT assay was performed as described above. IC₅₀ values of DOX were calculated from plotted results using untreated cells as 100%. The reversal fold, in terms of potency of reversal, was calculated using the following formula: reversal fold (RF) = IC₅₀ (MCF-7/DOX cells)/IC₅₀ (MCF-7/DOX cells combined with sample treatment). All assays were performed in triplicate.

References

- Zhan, Z. J., Ying, Y. M., Ma, L. F. & Shan, W. G. Natural disesquiterpenoids. *Nat. Prod. Rep.* **28**, 594–629 (2011).
- Paula, V. F., Rocha, M. E., Barbosa, L. C. A. & Howarth, O. W. Aquatidial, a new bis-norsesquiterpenoid from *Pachira aquatica* Aubl. *J. Braz. Chem. Soc.* **17**, 1443–1446 (2006).
- Toume, K. *et al.* Cytotoxic dimeric sesquiterpenoids from *Curcuma parviflora*: isolation of three new parviflorenes and absolute stereochemistry of parviflorenes A, B, D, F, and G. *Tetrahedron* **61**, 6700–6706 (2005).
- Li, Q. M. *et al.* Involucrastones A–C: unprecedented sesquiterpene dimers containing multiple contiguous quaternary carbons from *Stahlianthus involucratu*s. *Chem. Eur. J.* **21**, 13206–13209 (2015).
- Pingsusaen, P. *et al.* Investigation of anti-inflammatory, antinociceptive and antipyretic activities of *Stahlianthus involucratu*s rhizome ethanolic extract. *J. Ethnopharmacol.* **162**, 199–206 (2015).
- Hua, S. Z. *et al.* A pair of unique sesquiterpene-chalcone conjugates isolated from the seeds of *Alpinia katsumadai*. *Tetrahedron Lett.* **49**, 5658–5661 (2008).
- Hua, S. Z. *et al.* Two novel monoterpene-chalcone conjugates isolated from the seeds of *Alpinia katsumadai*. *Bioorg. Med. Chem. Lett.* **19**, 2728–2730 (2009).
- Yang, C. S. *et al.* A [2 + 2] cycloaddition dimer and a Diels-Alder adduct from *Alpinia katsumadai*. *Org. Lett.* **13**, 3380–3383 (2011).
- Yin, H. *et al.* Amomaxins A and B, two unprecedented rearranged labdane norditerpenoids with a nine-membered ring from *Amomum maximum*. *Org. Lett.* **15**, 1572–1575 (2013).
- Toume, K. *et al.* Parviflorenes B-F, novel cytotoxic unsymmetrical sesquiterpene-dimers with three backbone skeletons from *Curcuma parviflora*. *Tetrahedron* **60**, 10817–10824 (2004).
- Li, Q. M. *et al.* Involudispirones A and B: sesterterpenes containing a dispiro ring from *Stahlianthus involucratu*s. *Asian J. Org. Chem.* **4**, 1366–1369 (2015).
- Tanaka, N. *et al.* Bioulactones A–C, new pentacyclic meroterpenoids from *Hypericum chinense*. *Org. Lett.* **13**, 5488–5491 (2011).
- Gao, X. *et al.* Vibsatins A and B, two new tetranorvibane-type diterpenoids from *Viburnum tinus* cv. *variegatum*. *Org. Lett.* **16**, 980–983 (2014).
- Wilson, M. C. *et al.* Structure and biosynthesis of the marine streptomycete ansamycin ansalactam A and its distinctive branched chain polyketide extender unit. *J. Am. Chem. Soc.* **133**, 1971–1977 (2011).
- Seco, J. M., Quinoa, E. & Riguera, R. Assignment of the absolute configuration of polyfunctional compounds by NMR using chiral derivatizing agents. *Chem. Rev.* **112**, 4603–4641 (2012).
- Ohtani, I., Kusumi, T., Kashman, Y. & Kakisawa, H. High-field FT NMR application of Mosher's method. The absolute configurations of marine terpenoids. *J. Am. Chem. Soc.* **113**, 4092–4096 (1991).
- Ohtani, I., Kusumi, T., Kashman, Y. & Kakisawa, H. A new aspect of the high-field NMR application of Mosher's method. The absolute configuration of marine triterpene siphonol-A. *J. Org. Chem.* **56**, 1296–1298 (1991).
- Kusumi, T., Fujita, Y., Ohtani, I. & Kakisawa, H. Anomaly in the modified Mosher's method: absolute configurations of some marine cembranolides. *Tetrahedron Lett.* **32**, 2923–2926 (1991).
- Harada, N. & Nakanishi, K. The exciton chirality method and its application to configurational and conformational studies of natural products. *Acc. Chem. Res.* **5**, 257–263 (1972).
- Kobayashi, J. *et al.* Daphnocyclusins A–H, novel hexa- or pentacyclic alkaloids from two species of *Daphniphyllum*. *J. Am. Chem. Soc.* **123**, 11402–11408 (2001).
- Aoki, S. *et al.* Cortistatins A, B, C, and D, anti-angiogenic steroidal alkaloids, from the marine sponge *Corticium simplex*. *J. Am. Chem. Soc.* **128**, 3148–3149 (2006).
- Leverrier, A. *et al.* Kingianin A: a new natural pentacyclic compound from *Endiandra kingiana*. *Org. Lett.* **12**, 3638–3641 (2010).
- Zhu, H. C. *et al.* A pair of unprecedented cyclohexylethanoid enantiomers containing unusual trioxabicyclo[4.2.1]nonane ring from *Clerodendrum bungei*. *Tetrahedron Lett.* **55**, 2277–2279 (2014).
- Cheng, Z. B. *et al.* Extracellular signal-regulated kinases (ERK) inhibitors from *Aristolochia yunnanensis*. *J. Nat. Prod.* **76**, 664–671 (2013).
- Li, X. C., Elshohly, H. N., Nimrod, A. C. & Clark, A. M. Two auronols from *Pseudolarix amabilis*. *J. Nat. Prod.* **62**, 767–769 (1999).
- Zhan, Z. L. *et al.* Ternatusine A, a new pyrrole derivative with an epoxyoxepino ring from *Ranunculus ternatus*. *Org. Lett.* **15**, 1970–1973 (2013).

27. Wu, X. F. *et al.* Lysidicins F-H, three new phloroglucinols from *Lysidice rhodostegia*. *Org. Lett.* **12**, 2390–2393 (2010).
28. Joshi, P. R. *et al.* Regioselective synthesis of substituted arenes via aerobic oxidative [3 + 3] benzannulation reactions of α,β -unsaturated aldehydes and ketones. *Org. Lett.* **17**, 1449–1452 (2015).
29. Xue, J. H., Wu, P., Xu, L. X. & Wei, X. Y. Penicillitone, a potent *in vitro* anti-inflammatory and cytotoxic rearranged sterol with an unusual tetracycle core produced by *Penicillium purpurogenum*. *Org. Lett.* **16**, 1518–1521 (2014).
30. Park, H. B. *et al.* Spirobacillenes A and B, unusual spiro-cyclopentenones from *Lysinibacillus fusiformis* KMC003. *Org. Lett.* **14**, 5002–5005 (2012).
31. Chooi, Y. H. *et al.* Genome mining of a prenylated and immunosuppressive polyketide from pathogenic fungi. *Org. Lett.* **15**, 780–783 (2013).
32. Lee, Y. E., Cao, T., Torruellas, C. & Kozlowski, M. C. Selective oxidative homo- and cross-coupling of phenols with aerobic catalysts. *J. Am. Chem. Soc.* **136**, 6782–6785 (2014).
33. Tseng, Y. J. *et al.* Sinulochmodins A–C, three novel terpenoids from the soft coral *Sinularia lochmodes*. *Org. Lett.* **7**, 3813–3816 (2005).
34. Li, Q. M. *et al.* Sesquiterpenes from the rhizomes of *Alpinia japonica* and their inhibitory effects on nitric oxide production. *Fitoterapia* **86**, 29–34 (2013).
35. Xie, T. T. *et al.* Two novel abietane norditerpenoids with anti-inflammatory properties from the roots of *Salvia miltiorrhiza* var. *alba*. *Tetrahedron Lett.* **55**, 7106–7109 (2014).
36. Xia, Y. Z. *et al.* Schisandrin A enhances the cytotoxicity of doxorubicin by the inhibition of nuclear factor-kappa B signaling in a doxorubicin-resistant human osteosarcoma cell line. *RSC Adv.* **5**, 13972–13984 (2015).

Acknowledgements

This research work was supported by the Program for Changjiang Scholars and Innovative Research Team in University (IRT_15R63), the Project Funded by the Priority Academic Program Development of Jiangsu Higher Education Institutions (PAPD), and the Program for New Century Excellent Talents in University (NCET-12-0977).

Author Contributions

Q.-M.L. carried out the experimental work. J.-G.L., R.-Z.W., X.-B.W., M.-H.Y., J.L. and L.-Y.K. provided oversight. Q.-M.L., J.-G.L. and L.-Y.K. conceived the experiments and wrote the manuscript.

Additional Information

Supplementary information accompanies this paper at <http://www.nature.com/srep>

Competing financial interests: The authors declare no competing financial interests.

How to cite this article: Li, Q.-M. *et al.* Involucratins A–H: Unusual Cadinane Dimers from *Stahlianthus involucratus* with Multidrug Resistance Reversal Activity. *Sci. Rep.* **6**, 29744; doi: 10.1038/srep29744 (2016).



This work is licensed under a Creative Commons Attribution 4.0 International License. The images or other third party material in this article are included in the article's Creative Commons license, unless indicated otherwise in the credit line; if the material is not included under the Creative Commons license, users will need to obtain permission from the license holder to reproduce the material. To view a copy of this license, visit <http://creativecommons.org/licenses/by/4.0/>